Enhanced Australian carbon sink despite increased wildfire during the 21st century

Article

Published Version

It is advisable to refer to the publisher's version if you intend to cite from the work. See Guidance on citing.

www.reading.ac.uk/centaur

CentAUR

Central Archive at the University of Reading

Enhanced Australian carbon sink despite increased wildfire during the 21st century

D I Kelley[1] and S P Harrison[1,2]

[1] School of Biological Sciences, Macquarie University, North Ryde, NSW 2109, Australia
[2] School of Archaeology, Geography and Environmental Sciences, Reading University, Whiteknights, Reading, RG66AH, UK

E-mail: douglas.kelley@students.mq.edu.au

Abstract

Climate projections show Australia becoming significantly warmer during the 21st century, and precipitation decreasing over much of the continent. Such changes are conventionally considered to increase wildfire risk. Nevertheless, we show that burnt area increases in southern Australia, but decreases in northern Australia. Overall the projected increase in fire is small (0.72–1.31% of land area, depending on the climate scenario used), and does not cause a decrease in carbon storage. In fact, carbon storage increases by 3.7–5.6 Pg C (depending on the climate scenario used). Using a process-based model of vegetation dynamics, vegetation–fire interactions and carbon cycling, we show increased fire promotes a shift to more fire-adapted trees in wooded areas and their encroachment into grasslands, with an overall increase in forested area of 3.9–11.9%. Both changes increase carbon uptake and storage. The increase in woody vegetation increases the amount of coarse litter, which decays more slowly than fine litter hence leading to a relative reduction in overall heterotrophic respiration, further reducing carbon losses. Direct CO_2 effects increase woody cover, water-use efficiency and productivity, such that carbon storage is increased by 8.5–14.8 Pg C compared to simulations in which CO_2 is held constant at modern values. CO_2 effects tend to increase burnt area, fire fluxes and therefore carbon losses in arid areas, but increase vegetation density and reduce burnt area in wooded areas.

S Online supplementary data available from stacks.iop.org/ERL/9/104015/mmedia

Keywords: carbon cycle, fire regimes, CO_2 fertilization, water-use efficiency, dynamic vegetation modeling, future environmental changes

1. Introduction

Emissions from biomass burning are a significant contribution to the atmospheric carbon burden. Current estimates suggest that pyrogenic emissions are about 2.8 Pg C yr^{-1} (van der Werf *et al* 2006, van der Werf *et al* 2010) but may be as much as 3.4 Pg C yr^{-1} if small fires are included (Randerson *et al* 2012). For comparison, fossil fuel emissions and cement production contributed 8.3 ± 0.4 Pg C yr^{-1} to the atmospheric burden between 2002 to 2011 (Le Quéré *et al* 2014).

Interannual variability in wildfire contributes about one third of the variability in atmospheric CO_2 growth rate (Prentice *et al* 2011), and is driven by variability in climate—primarily caused by the El Nino Southern Oscillation (ENSO)—and its effect on the balance of fuel availability and combustibility (van der Werf *et al* 2006). Only about a fifth of the pyrogenic emissions globally are associated with deforestation fires (Bowman *et al* 2009, van der Werf *et al* 2010), and thus included in land-use for global budgeting purposes (Le Quéré *et al* 2014). Emissions from wildfires are not generally included in such budgets, because it is assumed that biomass-burning losses are compensated by post-fire uptake. If climate and fire regimes are in equilibrium, fire-induced atmospheric CO_2 emissions are approximately balanced by subsequent CO_2 uptake by surviving vegetation or via regeneration (Le

Quéré *et al* 2014). However, the uptake of carbon depends on how fast vegetation recovers versus fire frequency and intensity, and vegetation uptake will not necessarily balance pyrogenic emissions when climate is changing.

Climate projections for the 21st century (Collins *et al* 2013, Kirtman *et al* 2013) indicate that increases in temperature combined with reduced precipitation will increase fire risk in subtropical regions, precisely those areas most prone to wildfire today. Statistical modeling suggests that increased fire risk may not translate into increased burning because low fuel loads limit the amount of fire in some regions (Moritz *et al* 2012). However, statistical models do not account for potential changes in vegetation and their impact on fire regimes under a changing climate. Although fire-enabled vegetation models have been used to examine the impact of projected climate changes on the terrestrial biosphere (see e.g. Scholze *et al* 2006, Harrison *et al* 2010, Kloster *et al* 2012), there has been no vegetation model-based assessment of how changing climate will affect fire regimes, and hence the pyrogenic contribution to the carbon cycle, over the 21st century using the most recent climate scenarios.

Here we examine changes in the carbon cycle over the 21st century using a state-of-the art dynamic global vegetation model, LPX-Mv1 (Kelley *et al* 2014), driven by outputs from nine coupled ocean-atmosphere models in response to changes in forcing using the RCP4.5 and RCP8.5 scenarios, and focusing on Australia. Although Australia represents only about 6% of the global annual burnt area and contributes only about 5% of the total global emissions, most of these emissions (98%) are from wildfires in natural vegetation (Giglio *et al* 2013). This contrasts with other, more fire-prone continents such as Africa or Asia, where agricultural and deforestation fires contribute about 9% and 56% respectively of the fire-related emissions. Thus, Australia provides a good focus to examine the potentially complex interactions between vegetation and fire with changing climate and how these interactions could influence the regional carbon budget during the 21st century.

2. Methods

We examined the changes in the carbon cycle over the 21st century, driven by outputs from nine coupled ocean-atmosphere models in response to changes in forcing using two Representative Concentration Pathway (RCP) scenarios: RCP4.5 and RCP8.5. RCP4.5 is an intermediate radiative forcing (RF) scenario which stabilizes at $4.5 \, \mathrm{W m^{-2}}$ by 2100. RCP8.5 is an extreme RF scenario where RF reaches $8.5 \, \mathrm{W m^{-2}}$ by 2100 (see SI). In addition to the transient climate forcing, LPX-Mv1 is driven by atmospheric CO_2, which changes in the RCP4.5-driven simulations from 380.8 in 2006 to 576 ppm by 2080 CE and stabilizes thereafter (figure S3). In the RCP8.5 simulations, CO_2 concentrations increase throughout the 21st century to reach 1231 ppm by 2100. The robustness of the simulated changes is assessed by the agreement of the change between models using a one-sample *t*-test. The significance is measured by the strength of the

change relative to interannual variability in the historic period (1997–2006), as determined by the two-sample *t*-test. A change is described as 'robust' or 'significant' if the *t*-test *p*-value is <0.05 (see table S3 and S4). Changes in fluxes are assessed based on the averages for the last decade of the 21st century (2090–2099) compared to the last decade of the historical run (1997–2006), except that the carbon store is a measure of the accumulated change over the 21st century. The length of the comparison period was largely determined by the availability of burnt-area observations to evaluate the historical run. While a decade is sufficient to examine changes in the mean state, it precludes any consideration of the impact of longer-term (decadal) climate variability, which could nevertheless be important for understanding changes in Australian fire regimes.

Changes in the carbon cycle are simulated using the latest version of the land surface processes and exchanges dynamic global vegetation model (LPX-Mv1 DGVM: Kelley *et al* 2014. See SI for more information). This version of the model is a state-of-the-art process-based DGVM, which includes an adaptive treatment of bark thickness and of vegetation recovery after fire through resprouting. The improved treatment of vegetation responses to fire, makes LPX-Mv1 more suitable for analyses of climate-induced changes in the carbon cycle than the previously published version (Prentice *et al* 2011) which tended to over-predict burnt area in non-forest vegetation and to under-predict burnt area in forests.

LPX-Mv1 simulates vegetation dynamics using a set of 13 plant functional types (PFTs), defined by life form (tree, grass), where trees represent all woody plants (i.e. trees *sensu stricto* and shrubs), with the tree PFT further subdivided by leaf type, (broadleaf, needleleaf), phenological response to drought or cold (evergreen or deciduous), ability to resprout (resprouting, non-resprouting) and bioclimatic tolerance (tropical, temperate, boreal), and grasses subdivided by photosynthetic pathway (C_3, C_4). Fire is explicitly simulated as a function of lightning ignitions and fire susceptibility, calculated from fuel amount, fuel properties and fuel moisture content. The model does not simulate anthropogenic ignitions: except for deforestation fire, anthropogenic ignitions are not important for the large fires and hence burnt area which is the major determinant of the impact of fire on the carbon cycle. Fire spread, intensity and residence time are dependent on weather conditions (including wind speed) and fuel moisture, and calculated using the Rothermel equations (Rothermel 1972). The effective wind speed that influences fire spread is modulated by vegetation density in wooded areas, using a simple empirical relationship (Rothermel 1972). Thus, despite the fact that lightning ignitions are the sole source of fire starts, the timing of the fire season is predominantly determined by weather conditions. Burnt area is calculated as the product of the number of fires and fire spread. Mortality occurs through crown scorching or cambial death. Cambial damage is determined by fire intensity and residence time in relation to the bark thickness of local vegetation. The model includes a PFT-specific adaptive representation of bark thickness, in which the distribution of

bark thickness within an ecosystem changes in response to previous fire history. Fire fluxes are calculated using a standard emission factor for each trace gas species multiplied by the total amount of biomass burnt, which is the sum of dead and live fuel consumption as the result of surface fire and crown scorching. LPX-Mv1 uses a photosynthesis-water balance scheme that explicitly couples CO_2 assimilation with transpiration (see SI), where increased CO_2 leads to a fertilization effect that increases production in drier conditions. In common with most other vegetation models, LPX-Mv1 does not consider the effects of nutrient limitation on CO_2 fertilization.

LPX-Mv1 is run using monthly climate (maximum and minimum temperature, precipitation, cloud cover and number of wet days) from the CRU TS3.1 data set (Harris *et al* 2013) and wind speed from the National Center for Environmental Prediction (NCEP) reanalysis data (Kalnay *et al* 1996), interpolated to a daily timestep. Atmospheric CO_2 concentration is prescribed annually. The model was spun up using constant CO_2 (286 ppm), detrended climate data, and the cropland area of 1850 (table S1 in the supplementary data, available at stacks.iop.org/ERL/9/104015/mmedia), until the carbon pools were in equilibrium. The historical run used transient CO_2 from 1850 onwards. Detrended climate was used for all climate variables until 1900. From 1901 onwards, transient CRU TS3.1 was used for all climate variables except windspeed. Detrended wind speed is used until 1948 and transient values thereafter.

LPX-Mv1 was run from 2006 to 2100 using multiple climate realizations from climate model outputs in the CMIP5 database (table S2) forced by two alternative RCP scenarios (van Vuuren *et al* 2011): RCP4.5 and RCP8.5 (figure S1, figure S2). In the baseline runs, CO_2 was also allowed to vary (figure S3). Additional simulations were made in which climate was allowed to vary but CO_2 was held constant at the 2006 level of 380.8 ppm (fixed-CO_2 experiment). We made a further set of simulations with a version of the model in which resprouting was disabled (LPX-Mv1-nr: see Kelley *et al* 2014) in order to diagnose the impact of incorporating resprouting as a post-fire response (non-resprouting experiment). Ensemble averages of the outputs were created by simple averaging of the results of the appropriate set of individual simulations. The regional contributions to the overall changes shown in each experiment were diagnosed using geographic regions with similar vegetation types (figure S4), defined using k-means clustering.

The realism of the historic simulations was evaluated by comparing simulated and observed above-ground carbon (Ruesch and Gibbs 2008) and burnt area (GFED4: Giglio *et al* 2013). None of the simulations take account of land-use changes. However, for comparison of simulated and observed burnt area, cropland areas were masked out. Mapped values of observed above-ground biomass carbon (http://cdiac.ornl.gov/epubs/ndp/global_carbon/) are based on site-based measurements of above-ground biomass carbon. These are interpolated to land-cover types using a continent-specific interpolation based on vegetation composition and bioclimate.
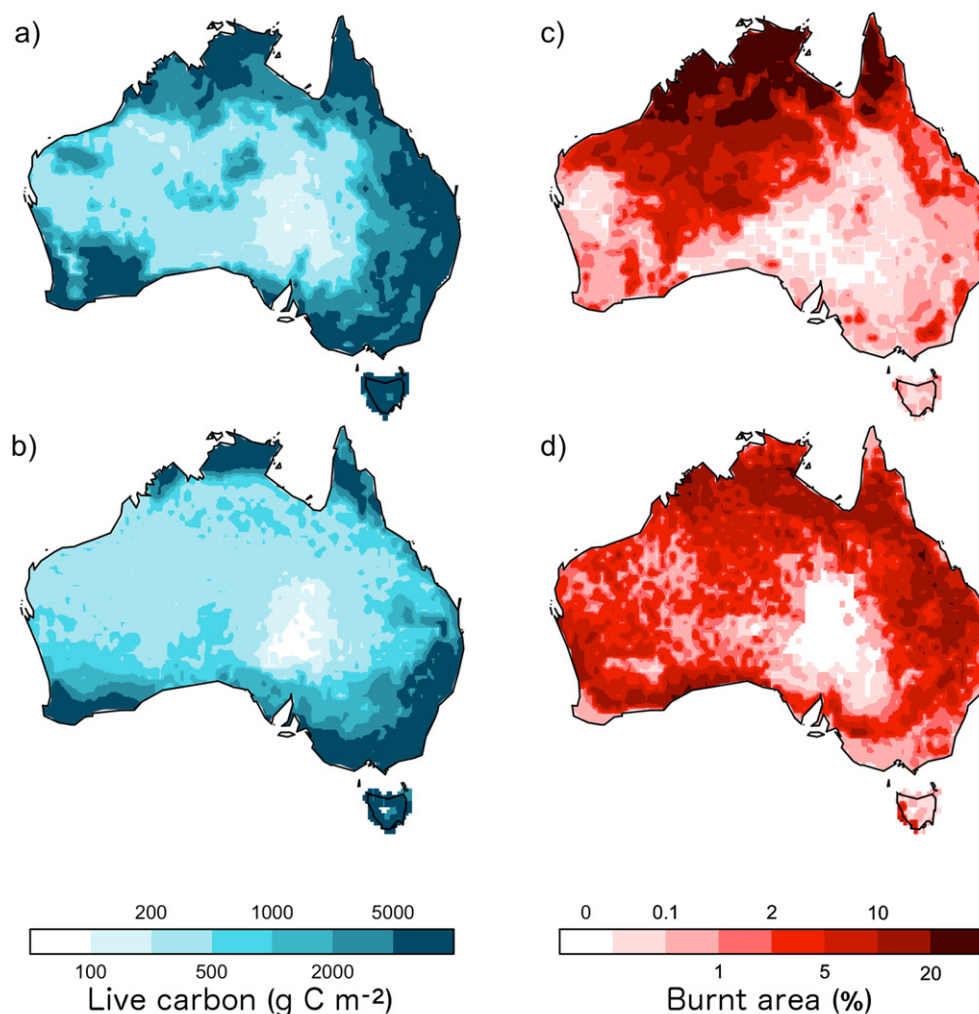
The average carbon biomass for a land-cover type in a specific continent was extrapolated over the GLC2000 5 × 5' land cover map (Bartholomé and Belward 2005). We excluded land areas described as swamps or anthropogenically-altered (e.g. urban or cropland) in GLC2000, and aggregated the remaining grid cells onto the 0.5° grid of LPX-Mv1. Aggregation was performed using the raster package in R (Hijmans 2014). We also compared the simulated net primary productivity (NPP), heterotrophic respiration (R_h) and fire fluxes during the historical periods with reconstructions of these fluxes derived from Haverd *et al* (2013) and GFED4 (Giglio *et al* 2013).

3. Results

3.1. Simulation of present-day carbon budget of Australia

Natural changes in the carbon stock are given by changes in NPP, heterotrophic respiration (R_h) and fire. Haverd *et al* (2013) have estimated the carbon budget of Australia between 1990 and 2011 by tuning a regional biosphere model (BIOS2) using observations of carbon and water fluxes, streamflow, and data on soil and vegetation carbon pools (Haverd *et al* 2013). Fire emissions for the period 1997–2009 were taken from GFED3 (van der Werf *et al* 2010), on the assumption that these values were representative of the longer period. Similarly, an estimate of harvest for 2004 was assumed to be representative for the whole period. Haverd *et al* (2013) estimated gross primary productivity as $4110 \pm 740 \, \text{Tg C yr}^{-1}$ and NPP as $2210 \, \text{Tg C yr}^{-1}$. Losses are dominated by heterotrophic respiration ($1997 \pm 383 \, \text{Tg C yr}^{-1}$), with smaller losses due to fire ($127 \pm 22 \, \text{Tg C yr}^{-1}$, which includes a component due to fires associated with land-use and clearing of $23 \pm 4 \, \text{Tg C yr}^{-1}$), harvest ($29 \pm 7 \, \text{Tg C yr}^{-1}$), land-use change ($18 \pm 7 \, \text{Tg C yr}^{-1}$), and riverine and dust transport ($3 \pm 1 \, \text{Tg C yr}^{-1}$). This budget suggests the continent gained carbon at an average rate of $36 \pm 29 \, \text{Tg C yr}^{-1}$ (net biosphere production) between 1990 and 2011. The gain in carbon is dominated by the effect of rising CO_2 ($68 \pm 7 \, \text{Tg C yr}^{-1}$; Haverd *et al* 2013). Increasing CO_2 directly influences the carbon cycle through CO_2 fertilization *sensu stricto*, improved water-use efficiency, and shifting the competitive balance of trees against grasses. Fire and land-use changes cause net respective losses of $26 \pm 4 \, \text{Tg C yr}^{-1}$ and $18 \pm 7 \, \text{Tg C yr}^{-1}$.

LPX-Mv1 reproduces the terms of the Australian carbon budget, within the limits of the estimation errors of each component and given uncertainties associated with differences in the time periods considered (figure 1). Our estimate of NPP ($2029 \, \text{Tg C yr}^{-1}$), based on the period 1997–2006, is comparable to Haverd *et al*'s estimate for 1990–2011 of $2210 \pm 398 \, \text{Tg C yr}^{-1}$ excluding the terms for harvest and land use, which are not simulated by our model. Our estimate for fire flux between 1997–2006 is slightly higher than that given by Haverd *et al* (2013) for the period 1997–2009 because the last three years of this period have low fire emissions. LPX-Mv1 also reproduces (figure 1) the large-scale geographic

Figure 1. Comparison of observed (a), (c) and simulated (b), (d) components of the carbon cycle during the recent period. Observed values for (a) above-ground biomass carbon for Australia were obtained from the Ruesch and Gibbs (2008) dataset (http://cdiac.ornl.gov/epubs/ndp/global_carbon/carbon_documentation.html). Observed average burnt area (c) for the period 1997 to 2006 is from GFED4 (Giglio *et al* 2013). Net primary productivity (NPP) and heterotrophic respiration (R_h) are averaged estimates for the period 1990 to 2011 from Haverd *et al* (2013). Observed fire flux is an average for the period 1997 to 2006 from GFED3 (van der Werf *et al* 2010). The simulated values are from the historic simulation, and are extracted for the appropriate years.

patterns of live carbon (Ruesch and Gibbs 2008), and burnt area from GFED4 (Giglio *et al* 2013); remaining biases in the simulated vegetation patterns or burnt area (Kelley *et al* 2014; see SI for further details) are small compared to simulated changes between the historic period and the end of the 21st century.

3.2. Response to RCP4.5 climate scenarios

The ensemble average climate shows a robust and significant increase in temperature over the 21st century, with an average increase of $2°C$ and increases of $>5°C$ in northwestern Australia (figure S5). There is a robust and marginally
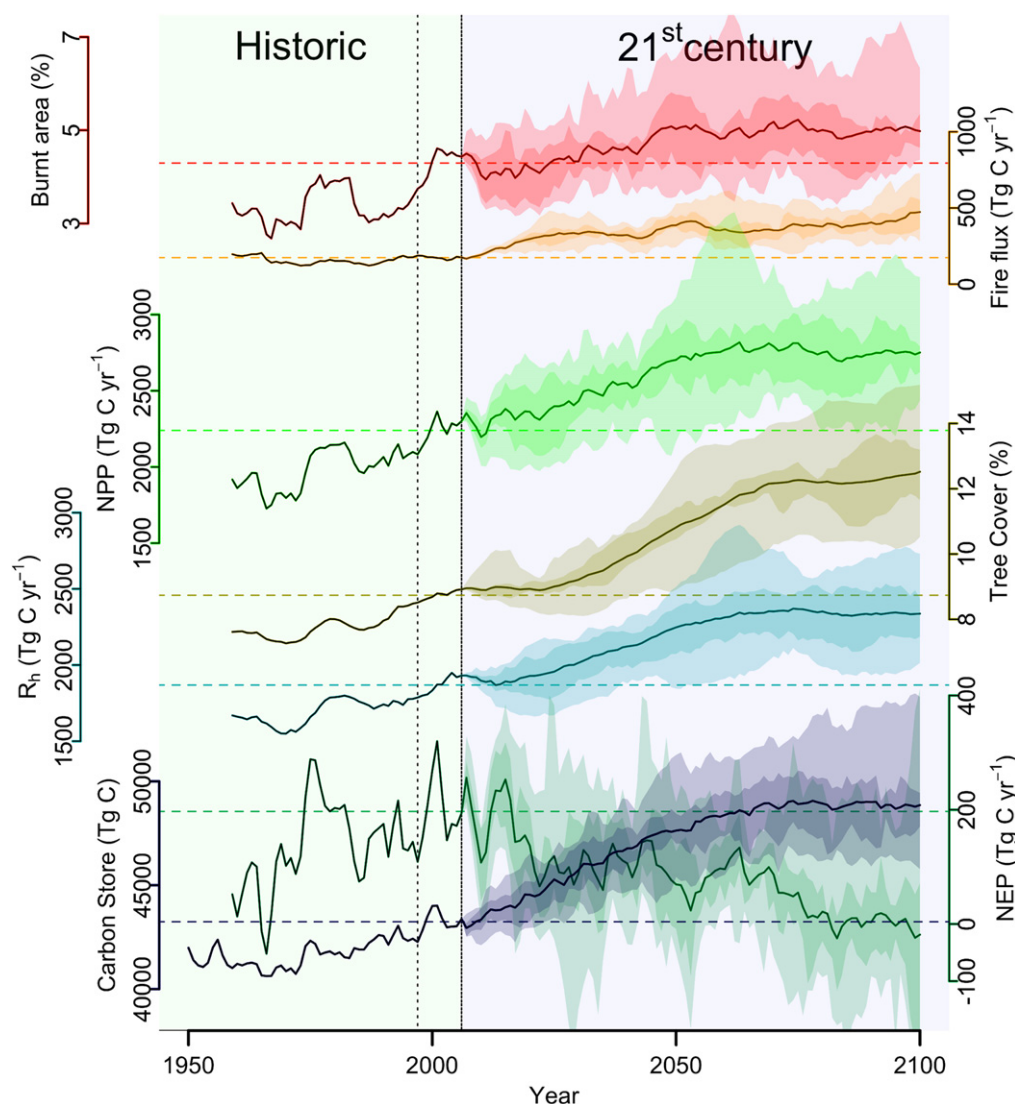
Figure 2. Changes in the carbon cycle over Australia through the 21st century in response to climate changes driven by the RCP4.5 scenario. The time series (bold lines) are ensemble averages of the model results for (a) burnt area (%), (b) fire flux (Tg C yr^{-1}), (c) net primary productivity (NPP) (Tg C yr^{-1}), (d) tree cover (%), (e) heterotrophic respiration (R$_h$) (Tg C yr^{-1}), (f) net ecosystem productivity (NEP) (Tg C yr^{-1}), and (g) carbon store (Pg C). The range in the individual model simulations is indicated by the shaded bands. The dashed horizontal lines indicate the average value of each variable during the last decade of the historic simulation.

Table 1. Summary of changes in individual components of the carbon cycle for Australia over the 21st century, based on ensemble averages of the simulations driven by the RCP4.5 and RCP8.5 climate scenarios. Robust changes are in bold, whilst significant changes are in italics.

Variable	Baseline			Fixed CO$_2$		Without resprouting		
	Historic	*RCP 4.5*	*RCP 8.5*	*RCP 4.5*	*RCP 8.5*	*Historic*	*RCP 4.5*	*RCP 8.5*
MAT (°C)	22	**24**	**26**	**24**	**26**	22	**24**	**26**
MAP (mm m^{-2} yr^{-1})	524	*491*	*485*	*491*	*485*	524	*491*	*485*
Burnt area (%)	5.32	**6.04**	**6.63**	4.74	**3.77**	5.66	**6.48**	**7.02**
Fire flux (Tg C yr^{-1})	169	**449**	**941**	166	141	120	**238**	**534**
NPP (Tg C yr^{-1})	2214	**2650**	**3448**	1982	**1706**	2190	**2559**	**3262**
Tree cover (%)	9.81	**13.71**	**21.75**	8.29	**6.32**	7.32	**10.07**	**16.77**
R$_h$ (Tg C yr^{-1})	1858	**2232**	**2709**	1756	1606	1857	**2263**	**2731**
NEP (Tg C yr^{-1})	189	−28	***−202***	62	−40	213	58	−3
Carbon store (Tg C)	41 607	**45 326**	**47 243**	36 842	32 453	33 972	**36 048**	**38 183**

significant decrease in precipitation in northern Australia of about 200 mm. Precipitation increases along the eastern coastal plains, in southeastern Australia and Tasmania, and also in southwestern Australia, but the changes are small, not robust and not significant. These climate changes drive an overall increase in burnt area, from $41 \, \text{Mkm}^2 \, \text{yr}^{-1}$ in the historic simulation to a multi-model mean value of $46 \, \text{Mkm}^2 \, \text{yr}^{-1}$ at the end of the century (table 1; figure 2). The change in burnt area leads to a 166% increase in fire flux, from $169 \, \text{Tg C yr}^{-1}$ in the historic simulations to $449 \, \text{Tg C yr}^{-1}$ by the end of the century. The increase in fire flux reflects an overall increase in biomass and particularly in woody biomass: NPP increases by $436 \, \text{Tg C yr}^{-1}$ over the 21st century and tree cover increases by 39%. However, net ecosystem productivity (NEP) remains largely positive (figure 2). Despite the increase in fire and the temperature-driven increase in heterotrophic respiration, there is an increase in the terrestrial carbon store, from $4.2 \, \text{Pg C}$ in the historic period to a multi-model mean value of $4.5 \, \text{Pg C}$ at the end of the 21st century (table 1; figure 2), with all but one of the simulations (MRI-CGCM3) showing an increase in carbon storage (table S3).

The regional contributions to this increase in carbon storage, and the pathways by which the increase occurs, vary. There is a significant decrease in fire in northern Australia because, despite the overall decrease in rainfall, more rain occurs in the fire season (May–October). Wetter fuels limit fire spread, an effect that is further enhanced by decreased wind speeds during the fire season. The reduction in fire is accompanied by an increase in tree cover, from 29% during the historic period to 56% by the end of the 21st century, and an increase in NPP by $28 \, \text{Tg C yr}^{-1}$. This increase in woody vegetation means that when fires do occur they release more carbon. Fire flux increases from $18 \, \text{Tg C yr}^{-1}$ to $124 \, \text{Tg C yr}^{-1}$ by the end of the century. As a result of this increase, northern ecosystems are converted from a sink before 2060 to a source after 2060 CE. Despite carbon losses in the latter part of the century, carbon storage is still $284 \, \text{Tg C}$ higher than during the historic period.

The interior of the continent is occupied by shrubland and open savanna, and experiences a large increase in fire over the 21st century. NPP increases from $1418 \, \text{Tg C yr}^{-1}$ to $1753 \, \text{Tg C yr}^{-1}$ and there is an increase in tree cover from 2% to 6% by the end of the century. Much of this region is fuel limited today, and the increased production and tree cover result in an increase in burnt area from 5% to 7%. However, the low biomass means the total increase in fire flux is small, from $52 \, \text{Tg C yr}^{-1}$ to $135 \, \text{Tg C yr}^{-1}$. This increase, combined with increased R_h (from $1222 \, \text{Tg C yr}^{-1}$ to $1522 \, \text{Tg C yr}^{-1}$) leads to a decrease in NEP during the century, although the region remains a sink throughout. As a result, there is an overall increase in the carbon stock, from $1.9 \, \text{Pg C}$ to $2.3 \, \text{Pg C}$.

The southern part of the continent experiences both increased and decreased fire, but the decreases are more important in magnitude and area. Much of this region is forested, with tree cover of >50%, and comparatively small changes in fire therefore have a large impact on the carbon

cycle. In areas characterized by small increases in fire, NPP increases during the first part of the century, from $311 \, \text{Tg C yr}^{-1}$ to $386 \, \text{Tg C yr}^{-1}$ by 2060, but then remains stable. Similarly, tree cover increases initially, reaching a maximum of 80% by 2060, and then decreases to 73% by the end of the century. Fire fluxes increase throughout the century, reaching $71 \, \text{Tg C yr}^{-1}$ by 2060 and $139 \, \text{Tg C yr}^{-1}$ by the end of the century. This region is a sink during the first half of the century, but NEP declines after 2060 because of increased fire and the shift towards less wooded biomes. Although the change in carbon stock between the end of the century and the historic period is small ($2.3 \, \text{Tg C}$), this reflects a large initial increase in carbon stock followed by a decrease of $1000 \, \text{Tg C}$ in the last 40 years. This large decline helps to explain why the continental budget shows little change in carbon stock during the latter part of the century. Only a comparatively small part of southern Australia experiences a decrease in burnt area over the 21st century. This decrease is not directly related to climate, since precipitation changes are not correlated with the change in fire, but results from increases in tree cover from 63% in the historic period to 79% by the end of the century. The increase in woody cover affects the ratio of fine to coarse fuel, which in turn affects fuel-drying properties resulting in an increase in fuel moisture throughout the year that limits fire spread. However, the increase in productivity and tree cover means that more carbon is released when fires do occur, so there is an overall increase in fire flux from $72 \, \text{Tg C yr}^{-1}$ to $101 \, \text{Tg C yr}^{-1}$. The combination of increased NPP (from $137 \, \text{Tg C yr}^{-1}$ to $157 \, \text{Tg C yr}^{-1}$) and decreased fires lead to a small increase in carbon store, from 4970 to $5105 \, \text{Tg C}$. These regions are a minor source today and become a net carbon sink from 2030 onwards.

Thus, although continental carbon stocks increase by $3.7 \, \text{Pg C}$, there are significant changes in regional sources and sinks over the 21st century. Regions characterized by an overall decrease in fire during the 21st century (i.e. northern Australia and parts of southern Australia) are sinks initially but become important sources in the latter part of the century. The continental interior is a sink throughout the 21st century. Although uptake is limited, the extent of this region means it contributes significantly to the end-of-century budget. Those parts of southern Australia where fire increases during the 21st century become a major source by the end of the century.

3.3. Response to RCP8.5 climate scenarios

The changes in climate in the RCP8.5 simulations are more extreme than in the RCP4.5 simulations. The ensemble average increase in MAT by the end of the 21st century is 4 °C, with larger changes in northwestern Australia. Although the average change in MAP is small, there is nevertheless a robust decrease in precipitation in northern and western Australia (ca $125 \, \text{mm yr}^{-1}$). The changes in burnt area are larger than in the RCP4.5 simulations. Fire flux increases from $169 \, \text{Tg C yr}^{-1}$ in the historic period to $941 \, \text{Tg C yr}^{-1}$ by the last decade of the 21st century (table 1; figure 3), more than double that of the RCP4.5 simulations. This increase in
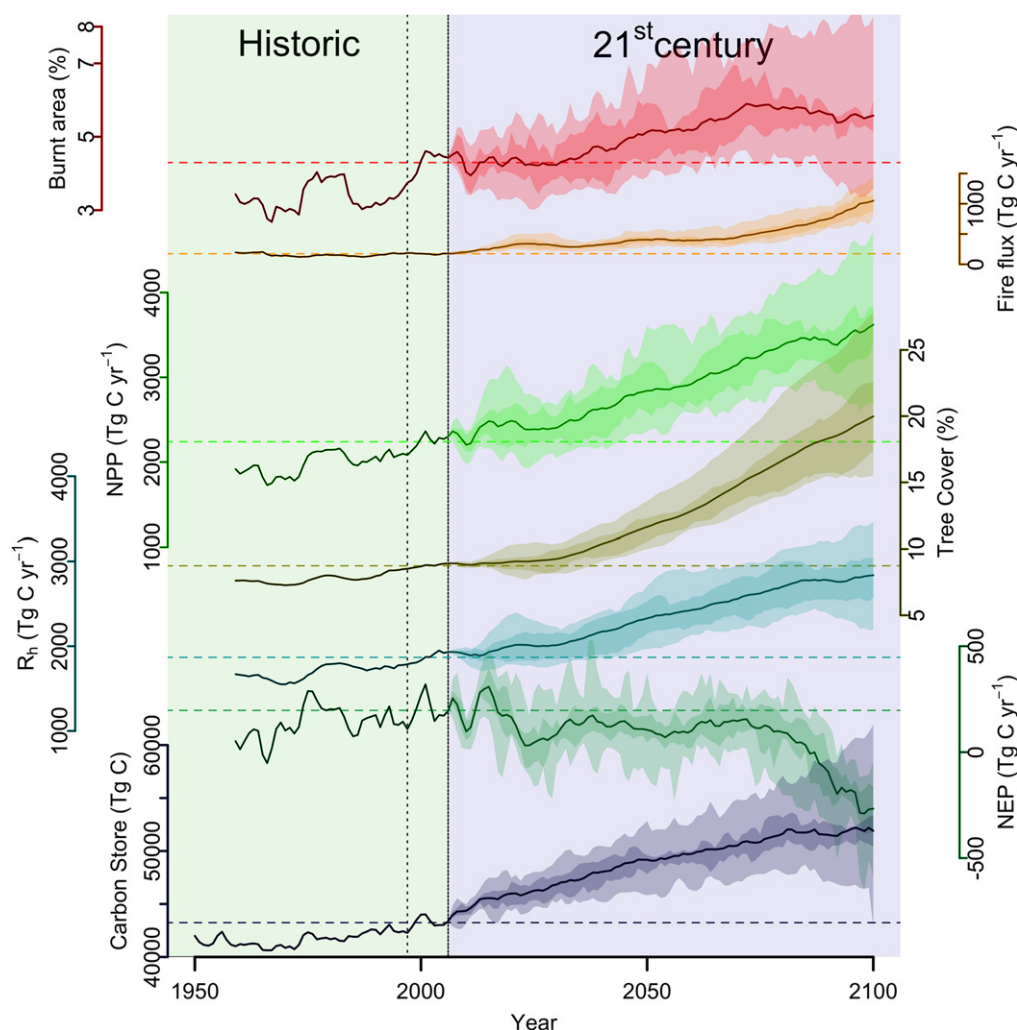
Figure 3. Changes in the carbon cycle over Australia through the 21st century in response to climate changes driven by the RCP8.5 scenario. The time series (bold lines) are ensemble averages of the model results for (a) burnt area (%), (b) fire flux (Tg C yr^{-1}), (c) net primary productivity (NPP) (Tg C yr^{-1}), (d) tree cover (%), (e) heterotrophic respiration (R$_h$) (Tg C yr^{-1}), (f) net ecosystem productivity (NEP) (Tg C yr^{-1}), and (g) carbon store (Pg C). The range in the individual model simulations is indicated by the shaded bands. The dashed horizontal lines indicate the average value of each variable during the last decade of the historic simulation.

fire flux is driven by a large increase in biomass and particularly woody biomass: NPP increases by 1234 Tg C yr^{-1} over the 21st century and tree cover increases by 122% compared to the historic run (table 1; figure 3). Although NEP is negative by the end of the century, the overall carbon store is increased by 5.6 Pg C at the end of the 21st century, a gain of 1.9 Pg C compared to the RCP4.5 simulations, and with all models showing an increase in carbon stores (figure S6; table S4).

The overall increase in carbon storage in these simulations is driven by changes in central Australia, where stocks increase by 7.1 Pg C by the end of the century. This increase reflects large increases in tree cover (14%) and NPP (950 Tg C yr^{-1}) and the fact that burnt area is only very slightly greater than in the RCP4.5 simulations (6.63% compared to 6.04%). Tree cover and NPP also increase in northern Australia. However, the reduction in fire compared to the historic period is less than in the RCP4.5 simulations,

because the decrease in precipitation is smaller, and as a result fire fluxes are large (233 Tg C yr^{-1} compared to 123 Tg C yr^{-1} in the RCP4.5 simulations). Thus, although northern Australia is characterized by an increase in carbon storage of 216 Tg C, this is less than in the RCP4.5 simulations. Those regions of southern Australia which experience increased fire during the 21st century, and thus increased fire fluxes, nevertheless also experience a significant increase in NPP. In contrast to the RCP4.5 simulations, carbon stocks increase throughout the century leading to an overall increase of 3.3 Tg C. The area of southern Australia that experiences reduced fire during the 21st century is smaller. The increase in NPP compared to the historic baseline is comparatively small (30 Tg C yr^{-1}) and these regions show a reduction in carbon stock (1 Pg C) by the end of the century. Although the continental interior is a sink throughtout the 21st century in the RCP8.5 simulations, both southern and northern Australia are sources by the end of the century.
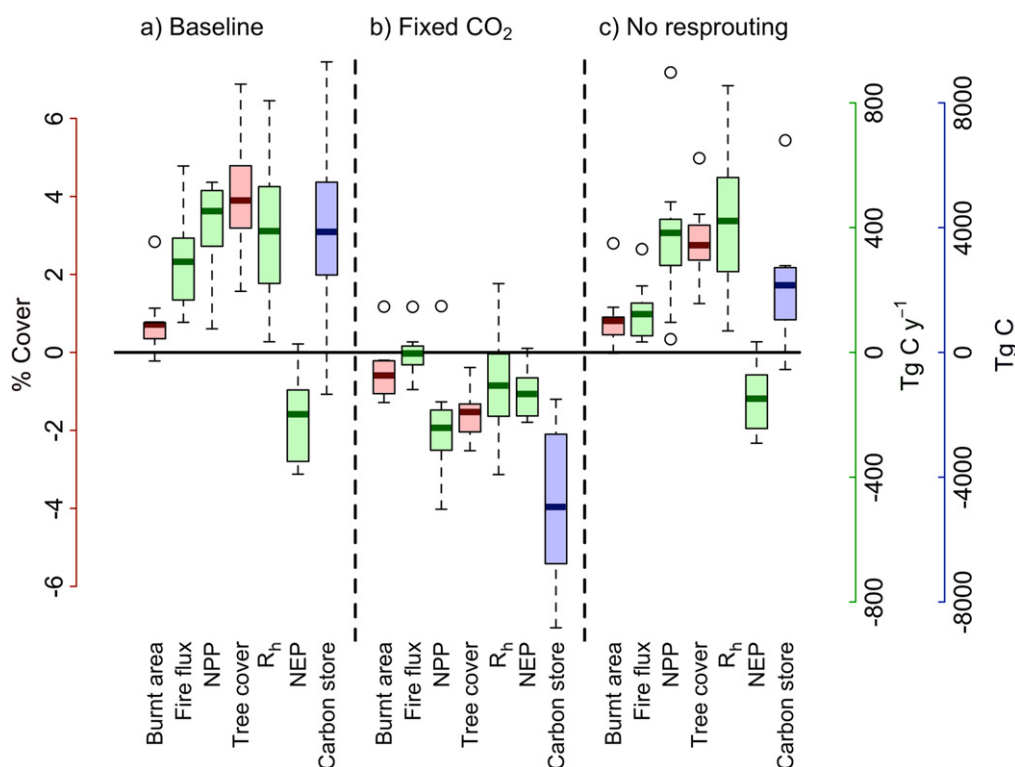
Figure 4. Contribution of CO_2 fertilization and resprouting to the simulated changes in the carbon cycle over the 21st century. The baseline plots (a) show the average changes in the last decade of the 21st century simulations relative to the 1997–2006 average from the historic simulation. The CO_2 plots (b) show the difference between the baseline 21st century run and a run in which CO_2 was fixed at 380.8 ppm (fixed CO_2). The no resprouting plots (c) shows the difference between the baseline 21st century run and the run in which resprouting was disabled. In the box-and-whisker plots, the solid lines show the mean value for the ensemble of simulations, the boxes show the interquartile range and the whiskers show the 5–95% confidence limits, and outliers are shown by an open circle. Note that the scale for carbon store is 10x that of the individual carbon components.

3.4. Impact of direct CO_2 effects on the 21st century carbon cycle

The inferred increase in carbon storage in Australia during the past two decades has been dominated by the effect of rising CO_2 (Haverd *et al* 2013). We evaluated the likely impact of rising CO_2 during the 21st century (figure S3), by running additional simulations in which CO_2 was held constant at 380.8 ppm (the 2006 value). We compare these simulations with the baseline simulation, in which both climate and CO_2 vary. NPP is decreased in the fixed-CO_2 RCP4.5 simulations compared to the historic period in all regions of the continent, and in contrast to the baseline simulations where NPP increases in all regions (figure 4, table 1). The impact of this difference varies regionally, reflecting the effects of the change on tree cover and fuel loads. Thus, in the continental interior, the increase in CO_2 produces increased vegetation cover and fuel loads, leading to an increase in burnt area and fire flux because of the removal of fuel limitations. A similar pattern is seen in regions in the south where changing climate reduces fire during the 21st century: the reduction in burnt area is smaller in the baseline simulations than in the fixed-CO_2 simulations because of additional production. Additionally, the CO_2-induced increase in NPP and in tree cover results in larger fire flux. In northern Australia, and those southern regions where 21st century climate changes reduce

fire, the increase in CO_2 increases both production and tree cover. This change in tree cover leads to an increase in coarse fuel, which in turn leads to slower fuel-drying times and an overall reduction in burnt area. Nevertheless, the fire flux is higher in both areas because the direct impact of CO_2 produces more material to burn. The overall and regional responses to CO_2 are similar and somewhat larger in the RCP8.5 simulations compared to the RCP4.5 simulations (table 1).

3.5. Impact of resprouting on the 21st century carbon cycle

The impact of fire on the carbon cycle and particular on carbon stocks is significantly different depending on whether the woody vegetation is fire-adapted. Most Australian ecosystems contain a significant proportion of trees that resprout after fire (Clarke *et al* 2013, Harrison *et al* 2014), ensuring rapid biomass recovery and persistence of woody vegetation in fire-prone regions. To examine the impact of resprouting on the Australian carbon budget, we ran both 21st century and historic simulations in which fire-affected trees were not allowed to resprout. The absence of resprouting leads to an overall decrease in carbon stock of 7.6 Pg C in the historic period compared to the standard run, which is unrealistically low. By the end of the 21st century, the carbon stock is 1.6 Pg C higher in the baseline RCP4.5 simulation than in the

simulation without resprouting (figure 4). The baseline simulation shows an increase in tree cover by the end of the 21st century, but despite the larger increase in burnt area in the baseline simulations, this increase is less without resprouting because fire-adapted trees are more likely to survive and indeed encroach into fire-prone areas. Except in the fuel-limited interior of the continent, the increased presence of trees reduces burnt area in the baseline simulations compared to the simulations without resprouting. This reflects the higher proportion of coarse fuel, which in turn increases fuel wetness. Although there are higher fire fluxes in the baseline simulations than in the simulations with no resprouting, because the amount of biomass is higher, the small increase in NPP associated with increased trees and the reduction in burnt area results in higher overall carbon storage when resprouting trees are present. Most of the additional carbon stock is in central (64%) and northern (22%) Australia: in the first case reflecting tree encroachment and in the second an increase in the abundance of resprouting trees. The regional impact of fire-adapted trees in southern Australia is less easy to diagnose because of the variability in the initial conditions between the baseline and non-resprouting simulations, coupled with the nonlinear nature of the carbon-cycle responses to changes in climate and fire, and the fact that a smaller proportion of species that occur today in the southern woodlands and forests are resprouters (Clarke *et al* 2013, Harrison *et al* 2014). Nevertheless, 13% of the overall increase in carbon storage is accounted for by the occurrence of fire-adapted trees in this region.

Similar results are shown in the RCP8.5 simulations (figure S6). In the absence of resprouting, with similar levels of burning overall, tree cover and NPP are reduced and the overall carbon stock at the end of the 21st century is 1.4 Pg C less than in the baseline RCP8.5 simulation. Thus, the presence of resprouting vegetation is important in maintaining high levels of tree cover and productivity in fire prone areas, and directly contributes to the overall increased carbon stock during the 21st century.

4. Discussion and conclusions

Our simulations show that fire will likely increase in Australia during the 21st century. This is consistent with the generally-accepted assumption that warmer and drier conditions will lead to an increase in fire risk (Williams *et al* 2001, Pitman *et al* 2007), although the increase in burnt area is perhaps less than might be expected because increased risk does not always translate into increased fire. The signal of increased fire is opposite to that predicted by Krawchuk *et al* (2009) using statistical modeling with a previous generation of climate projections, but similar in magnitude and pattern to predictions by Moritz *et al* (2012) using a similar approach and climate inputs to Krawchuk *et al* (2009).

Despite the increase in fire flux, and heterotrophic respiration, there is a large increase in carbon storage by the end of the 21st century. The general increase in NPP as a result of the direct impacts of CO_2 makes a significant

contribution to the increase in carbon stocks but the importance of fire-adapted trees in Australian ecosystems is also a contributing factor. Haverd *et al* (2013) have shown that CO_2 fertilization caused a 68 ± 15 Tg C yr^{-1} increase in carbon stock between 1990 and 2011. The rate simulated by LPX-Mv1 is slightly higher but nevertheless within the uncertainties of the estimated rate. One impact of increased CO_2 is to allow woody encroachment into semi-arid areas (Buitenwerf *et al* 2012, Bragg *et al* 2013, Donahue *et al* 2013), but these areas are fire prone and persistence of trees in these regions is only possible when they can resprout. Resprouting also affects fire regimes directly because the increased tree cover that such fire-adaptations permit in fire-prone regions leads to increases in the amount of coarse fuel, and therefore of fuel moisture, and decreased effective wind speed. Other things being equal, both of these will decrease fire spread and hence burnt area.

Our simulations suggest that the carbon cycle will be more vigorous over Australia during through the 21st century, with both increased uptake and increased fluxes. In the RCP4.5 simulations, NEP is positive during the first part of the century but shows no net change (NEP ≈ 0) during the last 20 years. As a result, although the carbon cycle is in equilibrium by the end of the century, carbon stock is increased by 10% compared to today. NEP is also positive during the first part of the century in the RCP8.5 simulations, but becomes negative after 2080 CE. Because the carbon sink in the first part of the century is much larger than in the RCP4.5 simulations, carbon stock is still larger than in the RCP4.5 simulations (14%) in the last decade of the century despite the fact that the continent becomes a significant carbon source.

The simulations presented here must be considered indicative rather than definitive statements about future fire-related changes in the carbon cycle. Clearly, the trajectory of future forcing is uncertain and our focus on the RCP4.5 and RCP8.5 scenarios therefore arbitrary. Furthermore, there are non-negligible inter-model differences in the climate response to these scenarios, particularly in interannual variability for key climate drivers of fire flux (figure S1). Further uncertainty is added by the use of a single fire-enabled DGVM, which has its own, known biases in the simulation of vegetation, fuel load and burnt area. Estimates of long term CO_2 fertilization maybe be reduced if nutrient limitation were considered, especially under the more extreme RCP8.5 scenario (Flato *et al* 2013). The point that we wish to emphasize is that the interaction between climate, fire and carbon dynamics is complex and nonlinear and not amenable to simple statements that increased fire (or fire risk) will reduce the terrestrial carbon sink.

Acknowledgements

Diagnosis and Intercomparison provides coordinating support and led development of software infrastructure in partnership with the Global Organization for Earth System Science Portals.) The analyses and figures are based on data archived by 18 June 2013. DIK is supported by an iMQRES at Macquarie University. We thank IC Prentice for comments on an earlier draft.

References

Bartholomé E M and Belward A S 2005 GLC2000: a new approach to global land cover mapping from Earth Observation data *Int. J. Remote Sens.* **26** 1959–77

Bowman D M J S *et al* 2009 Fire in the Earth system *Science* **324** 481–4

Bragg F *et al* 2013 n-Alkane stable isotope evidence for CO_2 as a driver of vegetation change *Biogeosciences* **10** 2001–10

Buitenwerf R, Bond W J, Stevens N and Trollope W S W 2012 Increased tree densities in South African savannas: >50 years of data suggests CO_2 as a driver *Glob. Change Biol.* **18** 675–84

Clarke P J *et al* 2013 Resprouting as a key functional trait: how buds, protection and resources drive persistence after fire *New Phytol* **197** 19–35

Collins M *et al* 2013 Long-term climate change: projections, commitments and irreversibility *Climate Change 2013: The Physical Science Basis. Contribution of Working Group I to the Fifth Assessment Report of the Intergovernmental Panel on Climate Change* ed T F Stocker *et al* (Cambridge: Cambridge University Press) www.ipcc.ch/report/ar5/wg1/

Donohue R J, Roderick M L, McVicar T R and Farquhar G D 2013 Impact of CO_2 fertilisation on maximum foliage cover across the globe's warm, arid environments *Geophys. Res. Lett.* **40** 3031–5

Flato G *et al* 2013 Evaluation of climate models *Climate Change 2013: The Physical Science Basis* 5th edned T F Stocker, D Qin, G-K Plattner *et al* (Cambridge: Cambridge University Press) pp 741–866 www.ipcc.ch/report/ar5/wg1/

Giglio L, Randerson J T and van der Werf G R 2013 Analysis of daily, monthly, and annual burned area using the fourth-generation global fire emissions database (GFED4) *J. Geophys. Res.-Biogeo.* **118** 317–28

Harris I, Jones P D, Osborn T J and Lister D H 2013 Updated high-resolution grids of monthly climatic observations–the CRU TS3.10 dataset *Int. J. Climatol.* **34** 623–42

Harrison S P, Marlon J R and Bartlein P J 2010 Fire in the Earth system *Changing climates, earth systems and society* ed J Dodson (Dordrecht: Springer) pp 21–48

Harrison S P *et al* 2014 Patterns in the abundance of post-fire resprouting in Australia based on plot-level measurements *Glob. Ecol. Biogeogr.* submitted

Haverd V *et al* 2013 The Australian terrestrial carbon budget *Biogeosciences* **10** 851–69

Hijmans R J 2014 Raster: geographic data analysis and modeling. R package version 2.2-31 http://CRAN.R-project.org/package=raster

Kalnay E *et al* 1996 The NCEP/NCAR 40-year reanalysis project *Bull. Am. Meteorol. Soc.* **77** 437–71

Kelley D I, Harrison S P and Prentice I C 2014 Improved simulation of fire–vegetation interactions in the Land surface Processes and eXchanges Dynamic Global Vegetation Model (LPX-Mv1) *Geosci. Model. Dev.* in press

Kirtman B *et al* 2013 Near-term climate change: Projections and predictability *Climate Change 2013: The Physical Science Basis. Contribution of Working Group I to the Fifth Assessment Report of the Intergovernmental Panel on Climate Change* ed T F Stocker *et al* (Cambridge: Cambridge University Press) www.ipcc.ch/report/ar5/wg1/

Kloster S, Mahowald N M, Randerson J T and Lawrence P J 2012 The impact of climate, land use, and demography on fires during the 21st century simulated by CLM-CN *Biogeosciences* **9** 509–25

Krawchuk M A *et al* 2009 Global pyrogeography: the current and future distribution of wildfire *PloS one* **4** e5102

Le Quéré C *et al* 2014 Global carbon budget 2013 *Earth Syst. Sci. Data* **6.1** 235–63

Moritz M A *et al* 2012 Climate change and disruptions to global fire activity *Ecosphere* **3** 1–22

Pitman A J, Narisma G T and McAneney J 2007 The impact of climate change on the risk of forest and grassland fires in Australia *Clim. Change* **84** 383–401

Prentice I C *et al* 2011 Modeling fire and the terrestrial carbon balance *Glob. Biogeochem. Cycles* **25** 1–13

Randerson J T *et al* 2012 Global burned area and biomass burning emissions from small fires *J. Geophys. Res.* **117** G04 012

Rothermel R C 1972 *A Mathematical Model for Predicting Fire Spread in Wildland Fuels* USDA Forest Service Research Paper INT-115 (Ogden, UT: Department of Agriculture, Intermountain Forest and Range Experiment Station)

Ruesch A and Gibbs H K 2008 *New IPCC tier-1 global biomass carbon map for the year 2000* (Oak Ridge, TN: Oak Ridge National Laboratory) Available online from the carbon dioxide information analysis center (http://cdiac.ornl.gov)

Scholze M, Knorr W, Arnell N W and Prentice I C 2006 A climate-change risk analysis for world ecosystems *Proc. Natl. Acad. Sci.* **103** 116–20

van der Werf G R *et al* 2006 Interannual variability of global biomass burning emissions from 1997 to 2004 *Atmos. Chem. Phys.* **6** 3423–41

van der Werf G R *et al* 2010 Global fire emissions and the contribution of deforestation, savanna, forest, agricultural, and peat fires (1997–2009) *Atmos. Chem. Phys.* **10** 11707–35

van Vuuren D P *et al* 2011 The representative concentration pathways: an overview *Clim. Change* **109** 5–31

Williams A, Karoly D and Tapper N J 2001 The sensitivity of Australian fire danger to climate change *Clim. Change* **49** 171–91